Dimensionally Stable Anode Based Sensor for Urea Determination via Linear Sweep Voltammetry

Maria de Lourdes S. Vasconcellos, Luiz Ricardo G. Silva, Chung-Seop Lee, Ana Sofia Fajardo, Sergi Garcia-Segura, Josimar Ribeiro

Dimensionally Stable Anode based sensor for Urea determination via Linear Sweep voltammetry

Maria de Lourdes Vasconcellos[1], Luiz Ricardo G. Silva[1], Chung-Seop Lee [2], Ana Sofia Fajardo[2,3], Sergi Garcia-Segura[2,*] and Josimar Ribeiro[1,*]

[1] Departamento de Química, Centro de Ciências Exatas, Universidade Federal do Espírito Santo, Av. Fernando Ferrari, 514, Goiabeiras, CEP: 29075-910, Vitória, ES, Brasil; maria.vasconcellos@edu.ufes.br, Luiz.silva@estudante.ufscar.br, josimar.ribeiro@ufes.br
[2] School of Sustainable Engineering and the Built Environment, Arizona State University, Tempe, Arizona 85287, United States; csleee@asu.edu , adossan3@asu.edu , sergio.garcia.segura@asu.edu
[3] Sorbonne Université, CNRS, Laboratoire Interfaces et Systèmes Electrochimiques (LISE), 4 place Jussieu, F-75005, Paris, France; adossan3@asu.edu
* Correspondence: josimar.ribeiro@ufes.br, sergio.garcia.segura@asu.edu

Abstract: Urea is an added value chemical with wide applications in industry and agriculture. Release of urea waste to the environment affects ecosystem health despite its low toxicity. Online monitoring of urea for industrial applications and environmental health is an unaddressed challenge. Electroanalytical techniques can be a smart integrated solution for online monitoring if sensors can overcome the major barrier associated to long term stability. Mixed metal oxides have shown excellent stability in environmental conditions with long lasting operational lives. However, these materials have been barely explored for sensing applications. This work presents a proof of concept that demonstrates the applicability of an indirect electroanalytical quantification method of urea. The use of Ti/RuO_2-TiO_2-SnO_2 dimensional stable anode (DSA®) can provide accurate and sensitive quantification of urea in aqueous samples exploiting the excellent catalytic properties of DSA® on the electrogeneration of active chlorine species. Cathodic reduction of accumulated HClO/ClO^- from anodic electrogeneration presented a direct relationship with urea concentration. This novel method can allow urea quantification with a competitive LOD of 1.83 x 10^{-6} mol L^{-1} within a linear range of 6.66 x 10^{-6} to 3.33 x 10^{-4} mol L^{-1} of urea concentration.

Keywords: Nitrogenated species, online monitoring, electroanalysis, chlorine reduction

1. Introduction

Urea is an important raw material for the chemical industry. Urea is widely used in fertilizers, animal food supplements, cosmetics production, and even in the pharmaceutical industry [1]. Despite the low-toxicity associated to urea, its undesired accumulation in the environment has been associated to soil acidification, eutrophication, groundwater pollution, and ammonia emissions to the air [2]. Therefore, online monitoring of urea is of the utmost importance not only for industrial processes but also for environmental health.

The determination of urea using nanoporous materials of metal oxides has been carried out by different techniques, such as Fourier transform infrared spectroscopy (FTIR), potentiometry, and conductometry [3-5]. However, the FTIR technique is not favorable to online monitoring. Regarding potentiometric and conductometric techniques, several studies report the development of biosensors. Considering that the elaboration of biosensors is more laborious, this study proposes a way to determine urea through indirect electroanalytical quantification. Electrochemical methods usually provide an easy way to deploy sensors with high sensitivity and moderately low cost [6]. Regarding potentiometric and conductometric techniques, most reports have focused on the study of biosensors. Biosensors provide direct measurement but suffer of low long-term stability. Considering that the elaboration of biosensors is more laborious, hence alternative approaches that are sturdy to environmental conditions are required.

Electroanalytical methods sometimes suffer of short-term stability resulting in single-use electrode probes, which is often considered a barrier for online monitoring. Metal oxide and mixed metal oxide electrodes are generating increasing interest due to their high stability and wide electrochemical window [7-9]. Metal oxide type sensors are excellent candidates for remote monitoring (online) and wireless applications, as they have a fast signal/response and long lifetime in different environmental conditions [7,9,10]. Mixed metal oxides have been mostly studied for electrochlorination and water treatment applications [6,7,12,13]. Several compositions are commercially available under the common denomination of Dimensionally Stable Anodes (DSA®) such as Ti/ RuO_2-TiO_2 [14-16]. The nature of the metal oxides and their ratio can modulate the desired electrocatalytic properties of DSA® electrodes and reduce their capital cost. Their properties are also directly related to their high proportion of surface/volume. Thus, the insertion of additional metal oxides in Ti/RuO_2-TiO_2 can enhance the competitiveness of commercial DSA® electrodes. That is the case

of tin oxide, a low-cost material with good catalytic activity [17,18]. Ti/RuO_2-TiO_2-SnO_2 electrodes synergistically integrate stability and sensing capabilities that can enable target analytes monitoring for water quality and industrial applications [7, 19-21].

DSA®-type electrodes have been widely studied in the literature [10,14-16,18]. To the best of our knowledge, there has not been any systematic investigation of the composition (Ti/RuO_2-TiO_2-SnO_2 (50:40:10 atom. %) reported in this paper in the literature. Moreover, the novelty is also associated to the indirect electroanalytical application of DSA®-type electrodes. Note that these materials are conventionally used in the chloro-alkali industry for manufacturing of chlorine and soda, but have not been reported as electrochemical urea sensors.

This work evaluates a novel indirect electrochemical method of urea quantification using a Ti/RuO_2-TiO_2-SnO_2 (50:40:10 atom. %) DSA®-type electrode. This proof of concept exploits the high electrocatalytic activity of DSA® on the electrogeneration of active chlorine species for indirect quantification of urea by linear sweep voltammetry based on the chlorine breaking point reaction of these nitrogenated species with chlorine. DSA®-type electrodes can produce chlorine from the electrochemical oxidation of chloride following reaction (1). Evolved chlorine quickly dissociates in water yielding hypochlorous acid according to reaction (2), which speciation is defined by the acid-base equilibria of reaction (3) [22, 23].

$$2\ Cl^- \rightarrow Cl_2 + 2\ e^- \quad (1)$$

$$Cl_{2(aq)} + H_2O \rightarrow HClO + Cl^- + H^+ \quad (2)$$

$$HClO \leftrightarrows ClO^- + H^+ \qquad pKa = 7.55 \quad (3)$$

Then, electrogenerated active chlorine species from the reactions (1)-(3) react with urea yielding N_2 as described from general expression (4) [17,24,25].

$$(NH_2)_2CO + 3\ ClO^- \rightarrow \quad N_2 + CO_2 + 3\ Cl^- + H_2O \quad (4)$$

This fast chemical reaction that consumes electrogenerated active chlorine species can be used to quantify the concentration of urea in solutions. This new indirect electrochemical method can contribute to enhance online monitoring of urea.

2. Materials and Methods

2.1. Electrode preparation

The electrode with nominal composition Ti/RuO_2-TiO_2-SnO_2 (Ru:Ti:Sn 50:40:10 atom. %) were prepared through thermal decomposition ($T_{calcination}$: 450°C). The polymeric film is subjected to high temperatures for the organic material is eliminated to obtain the oxide coating. Precursor solutions were prepared at the presence of 0.1 mol of $RuCl_3$, $C_{12}H_{28}O_4Ti$, and $SnCl_4$ (all Sigma-Aldrich), in ethanol. After, the precursor mixtures were dissolved at the presence of the 4.0 mol acid citric and 16.0 mol ethylene glycol (all Sigma-Aldrich) and heated at T= 90°C to occurred esterification process. Before the deposition of oxide films, the plate of titanium (2.0 cm^2) used as substrate was sandblasted (105 - 210 μm) in order to improve the adherence of metal oxides. After that, the surface was degreased and submitted to chemical activation in concentrated HCl (20 % v/v) for 30 minutes, washed in a solution of oxalic acid (10%) for 20 minutes, and rinsed with ultrapure water. Afterwards, the electrode was dried at low temperature. The precursor mixtures were deposited on the pretreated Ti substrate. The deposited coatings were thermally treated in the oven at 130°C for 10 minutes, the again at 450°C for 5 minutes. Upon reaching the desired mass, the electrode was calcined at 450°C for 1 hour.

2.2. Sample preparation

The synthetic urine sample was prepared according to literature [26-28]. Thus, 4.98 x 10^{-2} mol L^{-1} of NaCl, 2.14 x 10^{-2} mol L^{-1} of KCl, 14.48 x 10^{-3} mol L^{-1} of $CaCl_2.H_2O$, 15.76 x 10^{-3} mol L^{-1} of Na_2SO_4, 10.28 x 10^{-3} mol L^{-1} of KH_2PO_4, 18.7 x 10^{-3} mol L^{-1} of NH_4Cl, and 0.416 mol L^{-1} of urea were added in ultrapure water. The analyses of synthetic urine samples were conducted in diluted urine solutions containing 2. 77 x 10^{-4} mol L^{-1} of urea in 0.10 mol L^{-1} KCl.

2.3. Physicochemical characterizations

The surface morphology and elemental composition of the deposited oxide films were analyzed by X-ray diffraction (XRD) and scanning electron microscopy coupled with energy dispersive X-ray spectroscopy (SEM-EDS, FEI Philips XL-30). The XRD analyses were performed using a Bruker D8 diffractometer operating with Cu Kα radiation (λ = 1.5406 Å), with a 2θ scan of 10° to 90° (0.01° min^{-1}) operating at 40 kV voltage and 40 mA current. The apparent size of the crystallite was estimated using the Scherrer equation [29] for all the diffraction planes.

$$D = 0.9\lambda / (\beta \cos\theta_\beta) \quad (5)$$

where D corresponds to the apparent size of the crystallite, λ to the wavelength of the radiation, β to the diffraction full width at half-maximum intensity (FWHM) and θ_β to the angle at maximum intensity and the wavelength.

2.4. Electrochemical characterizations

All solutions were prepared using ultrapure water with resistivity of 18.2 MΩ cm at 22 °C. For the electrochemical measurements, a 30 mL electrochemical cell was used with an Ag/AgCl reference electrode with saturated KCl solution, a counter electrode of carbon graphite with an area of 3.15 cm^2 and a working electrode Ti/RuO_2- TiO_2-SnO_2 (Ru:Ti:Sn 50:40:10 atom. %) with an area of 1.5 cm^2.

The catalytic sites of the working electrode were activated by cyclic voltammetry (CV) were carried out with a potentiostat/galvanostat AUTOLAB model 302 during 50 consecutive cycles at a scan rate of 50 mV s^{-1} in the supporting electrolyte HCl 1.0 mol L^{-1}. After the activation, all experiments were conducted in KCl 0.10 mol L^{-1} as a supporting electrolyte. We adapted previous know-how of our group and scientific literature on the electrochemical characterization of DSA®-type electrodes by cyclic voltammetry [19,22,30]. Furthermore, we conducted preliminary tests to better define the analysis parameters, e.g., conditioning time, linear range, scan rate, and pre-cleaning. No poisoning nor fouling effects were observed under experimental conditions for several consecutive cycles, that showed reproducible values of analyte concentration.

The voltammetric charge can be used as a relative measure of the electrochemically active area. The voltammetric charge (q) is used to evaluate the electrochemically active area of noble metal oxide electrodes. It is obtained through the integration of the cyclic voltammogram characteristic of the electrode and it is proportional to the number of active sites [30,31]. Therefore, the anodic and cathodic charge densities, q_a and q_c, were determined by integration of region of the i versus E curve measured between 0.2-1.0 V vs. Ag/AgCl (q_a = 13.66 mC cm^{-2} and q_c = 13.05 mC cm^{-2}). The influence of chlorine active species was assessed by conducting experiments in inert electrolyte consisting of 0.033 mol L^{-1} Na_2SO_4 solutions in absence and presence 2.68 x 10^{-3} mol L^{-1} NaClO.

The quantification of urea was obtained from the peak cathodic current. The measurements of linear sweep voltammetry (LSV) were carried out with a potentiostat/galvanostat AUTOLAB model 302. LSV analyses started with a 60 second preconditioning time at 1.2 V vs. Ag/AgCl and followed by a cathodic scan from 1.2 V to 0.2 V vs. Ag/AgCl at 50 mV s−1 scan rate. The concentrations of urea ranged from 6.66 x 10^{-6} to 3.33 x 10^{-4} mol L^{-1}.

For interference tests, a study with different metal ions such as: Iron(III), nickel(II), zinc(II), cadmium(II), copper(II), sulfur(II), lead(II) and mercury(II) (all Sigma-Aldrich) was performed. All interferents were studied at 1:1 ratio. The 1:1 ratio used was 2.0 x 10^{-5} mol L^{-1} for interferent and urea, respectively.

3. Results and discussion

3.1. Physicochemical characterizations of Ti/RuO_2-TiO_2-SnO_2

The structure of the synthesized electrosensing Ti/RuO_2-TiO_2-SnO_2 films were analyzed by XRD. Figure 1 illustrates the crystal structure of the DSA® film deposited on the titanium substrate. The characterization shows the presence of metallic titanium (PDF- 44-1294) associated to the titanium support, whose peaks were displaced to slightly greater values of 2θ due to the joint contribution of the three metals that introduce cell distortion. The diffractogram allows clearly identifying characteristic peaks associated to the tetragonal crystalline phase of RuO_2 (PDF- 40-1290), and the anatase structure of TiO_2 (PDF- 21-1272). Characteristic peaks associated to SnO_2 were not observed due to the low content of this metal in the mixed-metal oxide composition. The absence of peaks suggested the formation of a solid solution following the Hume-Rother rule as have been observed in other mixed metal oxide compositions [16,24]. This common behavior is explained by the small difference in the ionic radius of the elements Ru^{4+} (0.062 nm), Ti^{4+} (0.060 nm), and Sn^{4+} (0.069 nm) that did not exceed 15%; which induces the substitution solid solution in the titanium structure [19,32-34].

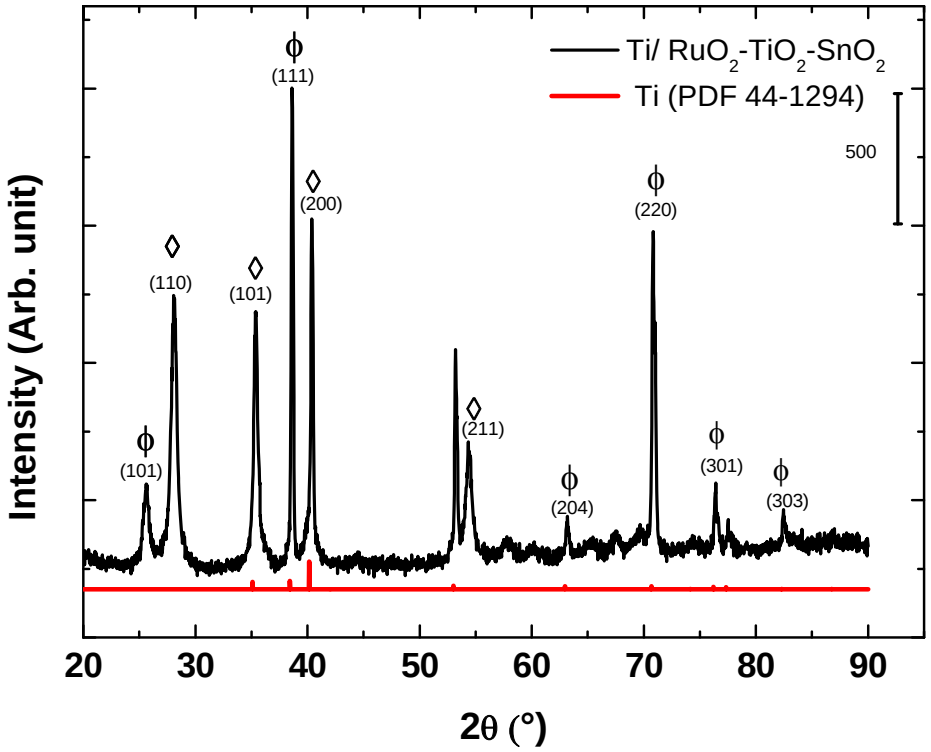

Figure 1. XRD pattern for the DSA® Ti/RuO_2-TiO_2-SnO_2 (50:40:10 atom. %): (Φ) RuO_2 tetragonal; (◇) TiO_2

From the XRD data, the apparent crystallite size was calculated and summarized in Table 1. When comparing Table 1 to the apparent size of the crystallite values for solid solution RuO_2 and TiO_2 phase, the result implies that the ruthenium oxide might be incorporating titanium/tin atoms in their crystalline lattice and thus distorting the structure of TiO_2.

Table 1. Apparent size of the crystallite (D) obtained for the DSA® Ti/RuO_2-TiO_2-SnO_2 (50:40:10 atom. %) electrode on different phases.

	D (nm)								
	(101)	**(110)**	**(200)**	**(211)**	**(111)**	**(204)**	**(220)**	**(301)**	**(303)**
Solid solution	20	15	38	17.	-	-	-	-	-
TiO_2 phase	16	-	-	-	44	29	28	26	31

The surface morphology and the composition of the formed films were analyzed using the SEM and EDS techniques. Figure 2a depicts the characteristic electrode surface morphology of DSA® electrodes with a mud cracked structure [29,34]. The EDS analyses of Figure 2b allowed identifying signals for the three metals in the mixed metal oxide composition of Ti/RuO_2-TiO_2-SnO_2 (50:40:10 atom. %). The EDS demonstrates the presence of Sn in the electroactive film despite of not having observed an associated crystalline structure in XRD (see Fig. 1), which allows inferring its solid solution in TiO_2 and RuO_2. Table 2 collects the atomic composition determined through EDS analyses, and indicates a good correlation between experimental and nominal compositions. Thus, the DSA preparation method effectively formed a mixed metal oxide film from the polymer precursor calcination.

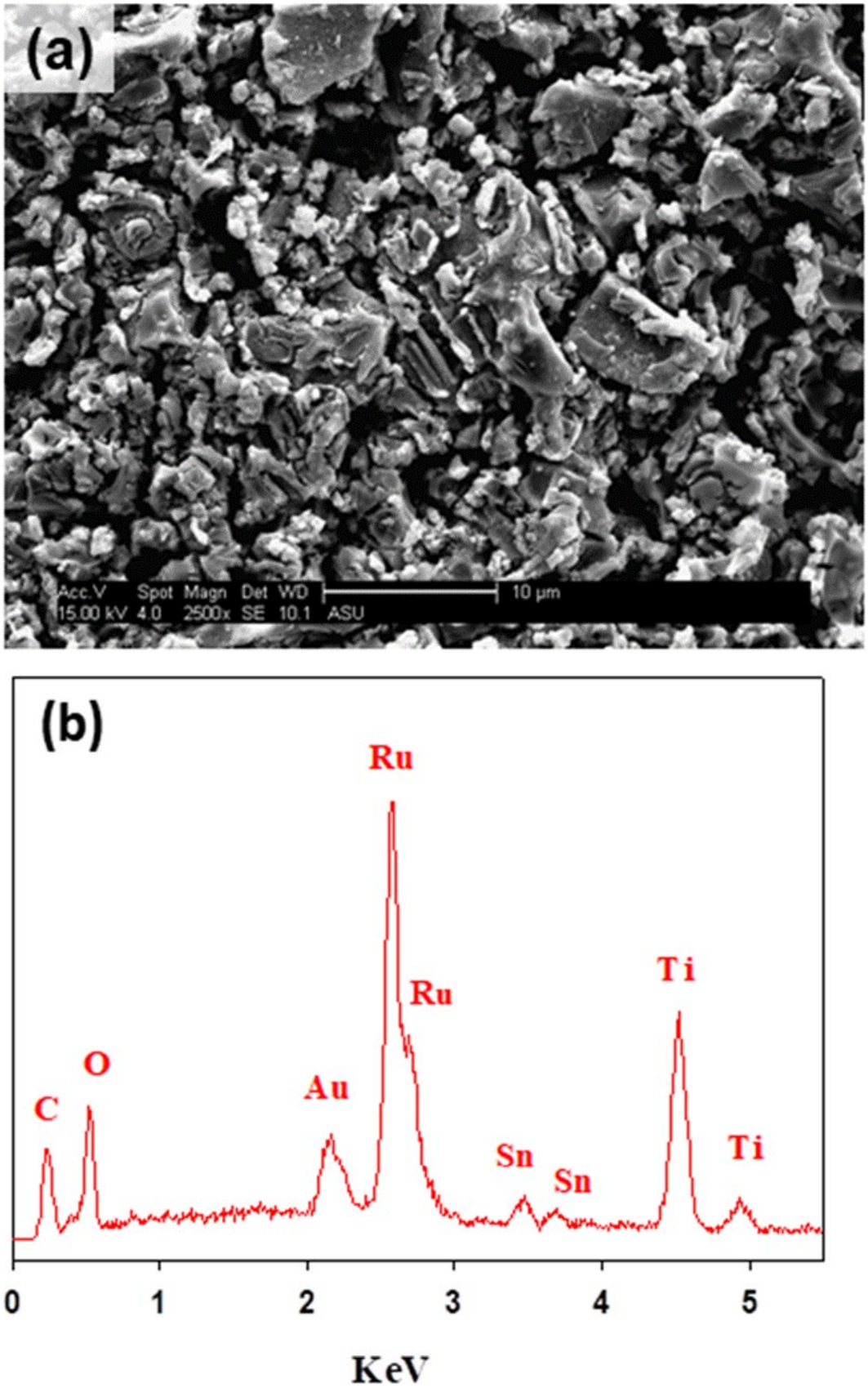

Figure 2. (a) SEM image of the DSA Ti/RuO_2-TiO_2-SnO_2 (50:40:10 atom. %) and (b) EDS spectrum.

Table 2. Elemental composition of DSA electroded defined by Energy Dispersive X-Ray Spectroscopy (EDS). Experimental composition is describred in atomic percentage as usually used to describe elemental composition of electrodic materials.

Nominal composition (atom. %)	**Experimental composition (atom. %)**		
	Ru	**Ti**	**Sn**
Ti/RuO_2-TiO_2-SnO_2 (50:40:10 atom. %)	45	50	4.7

3.2. *Electrochemical characterizations*

The electroanalytical behavior of the DSA as working electrode is shown in Figure 3. The CV analysis of Ti/RuO_2-TiO_2-SnO_2 in Na_2SO_4 supporting electrolyte at pH 7.0 shows an increase in current response at 1.1 V vs. Ag/AgCl that is associated to oxygen evolution reaction (OER) from water oxidation. The onset potential of OER shows an overpotential (η) of 1.0 V which is commonly associated to active electrodes [14]. When CV is conducted in KCl as a supporting electrolyte under identical ionic strength of 0.10 two peaks were observed (see Figure 4). The peak located in the region between 0.10 – 0.70 V vs. Ag/AgCl was attributed to Ru(III)/Ru(IV) redox transition. Meanwhile, the second peak in the region between 0.8 – 1.1 V vs. Ag/AgCl was attributed to Ru(IV)/Ru(VI) redox transition [33,34]. In the region from 1.0 V vs. Ag/AgCl the start of the chlorine evolution reaction (ClER) an increase is observed in the current response that is associated to the coexistence of chloride oxidation reaction (1) and water oxidation (*i.e.*, OER) [33,34]. The most notorious difference is the clear reduction peak observed in the cathodic scan that is ascribed to the reduction of active chlorine species electrogenerated during the anodic scan. To demonstrate that the cathodic peak observed in presence of chloride is indeed associated to the cathodic reduction of ClO^-, a blank experiment in Na_2SO_4 supporting electrolyte containing 2.68 x 10^{-3} mol L^{-1} of NaClO was carried out. Under these conditions the reduction peak appeared at the same potential of 1.0 V vs. Ag/AgCl demonstrating that this charge transfer process is actually associated to ClO^- cathodic reduction.

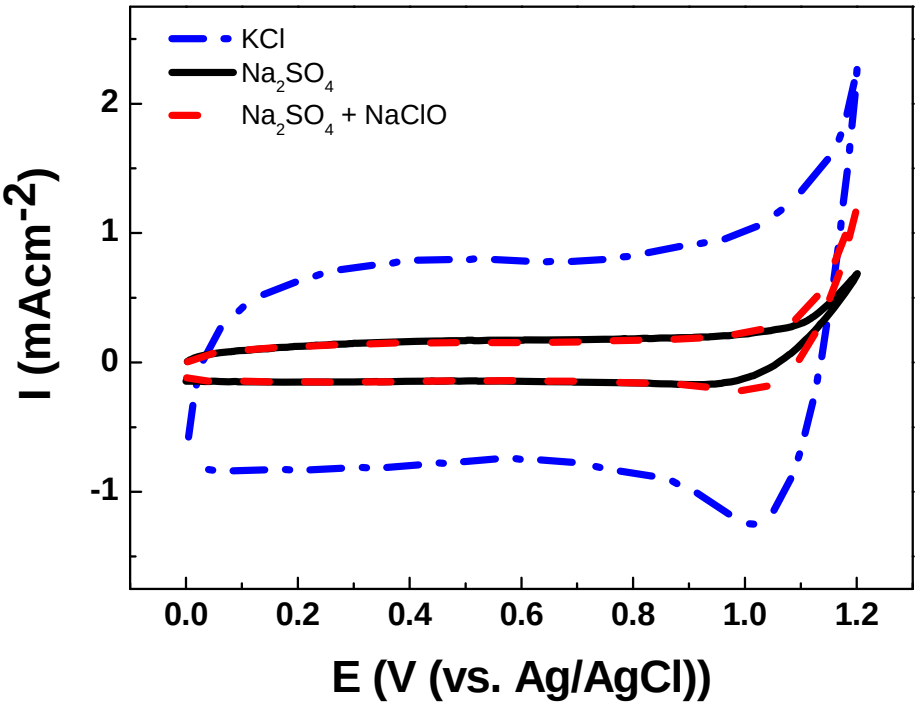

Figure 3. Cyclic voltammetry of Ti/RuO_2-TiO_2-SnO_2 (50:40:10 atom. %) as working electrode at υ = 50 mVs^{-1} scan rate in (—.—) 0.1 mol L^{-1} KCl solution, (—) 0.033 mol L^{-1} Na_2SO_4 solution, and (— —) 0.033 mol L^{-1} Na_2SO_4 in the presence of NaClO 2.68 x 10^{-3} mol L^{-1} at pH 7.0 and T = 24 °C.

The reduction peak observed is a key aspect for the indirect electrochemical quantification of urea since the concentration of the target analytes can be indirectly estimated from the $HClO/ClO^-$ consumed by the chemical reactions (2) and (3). Figure 4 illustrates how the presence of urea decreases the intensity of the cathodic peak associated to the reduction of $HClO/ClO^-$. This trend is associated to the lower accumulation of active chlorine species in the solution due to their consumption by fast chlorine breaking point chemical reactions.

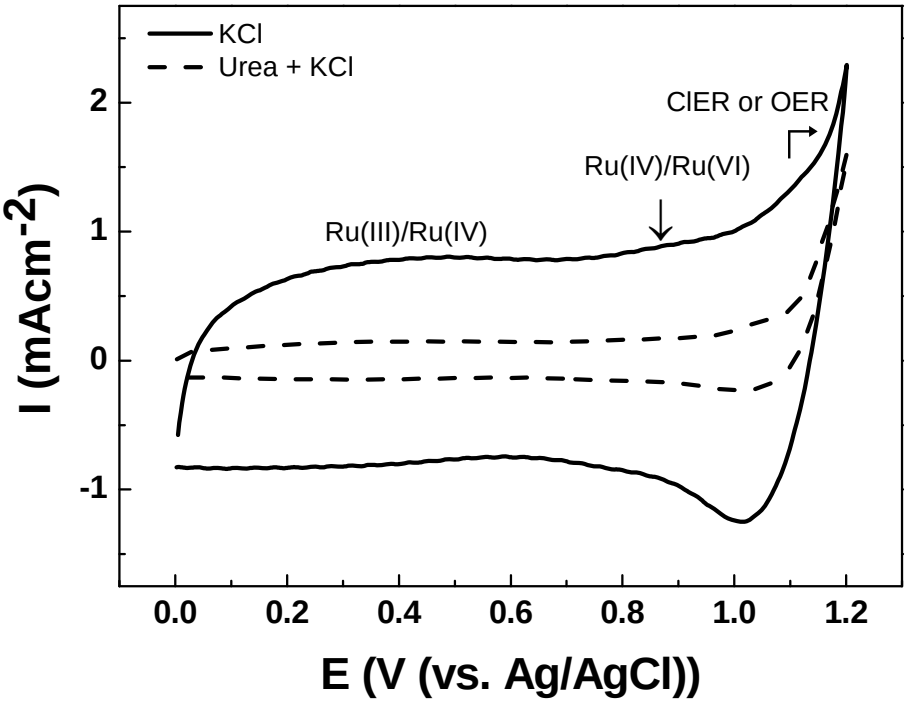

Figure 4. Cyclic voltammetry registered in 0.10 mol L^{-1} KCl solution in (—) absence of urea, and(---) in the presence of 3.33 x 10^{-4} mol L^{-1} of urea Ti/RuO_2-TiO_2-SnO_2 (50:40:10 atom. %) as working electrode at υ = 50 mVs^{-1} scan rate at pH 5.3 ± 0.1 and T = 24 °C.

The cathodic charge densities (q_c) determined in the different solutions tested are collected in Table 3. It can be seen that the q_c-values obtained for the solutions of urea showed a q_c reduction of 88% in relation to (q_c) KCl solution value. This electrochemical response is related to the amount of non-consumed HClO remaining in solution.

Table 3. Collected q_c-values obtained at the range of 0.8 – 1.1 V vs. Ag/AgCl for DSA Ti/RuO_2-TiO_2-SnO_2 (50:40:10 atom. %)

Solution	Cathodic charge density, q_c (mC cm^{-2})
Na_2SO_4	0.0
KCl	9.4
Na_2SO_4 with NaClO	1.0
Urea in KCl	1.1

LSV analyses were conducted to determine the relationship between the cathodic peak intensity and the concentration of urea in solution. Initial potential of 1.2 V vs. Ag/AgCl was hold for 60 s to ensure the electrogeneration of active chlorine species required for the analyses. Thereafter, the current response was registered during the negative-going scan from 1.20 to 0.20 V vs. Ag/AgCl. The LSV readings registered for urea concentrations ranging between 6.66 x 10^{-6} to 3.33 x 10^{-4} mol L^{-1} of urea are depicted in Figure 5a. Interestingly, it can be observed that the cathodic peak intensity decreases while increasing the concentration of urea in solution. The cathodic peak intensity (I_{peak}), which is related to urea concentration, presented a linear relationship with R^2 = 0.997. From the slope of the analytical curve, the limits of detection and quantification were calculated according to the formulas: LOD = (3 × SD_{blank})/Slope and LOQ = (10 × SD_{blank})/Slope. Where SD blank is the standard deviation of 10 voltametric measurements of blank and slope of the

analytical curve [37], which are summarized in Table 4. Low LOQ of 7.66 x 10^{-6} mol L^{-1} encourage the possible application of this indirect method for the quantification of urea.

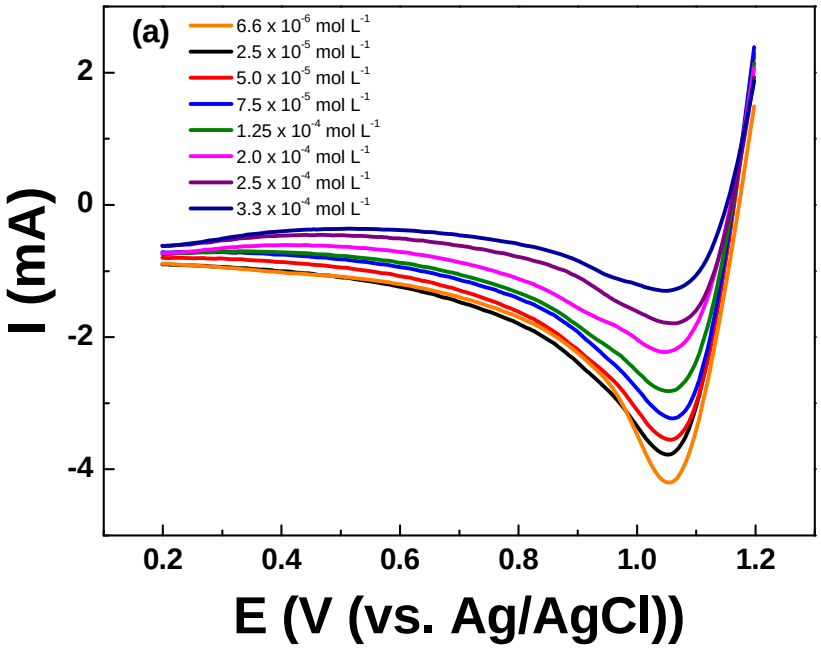

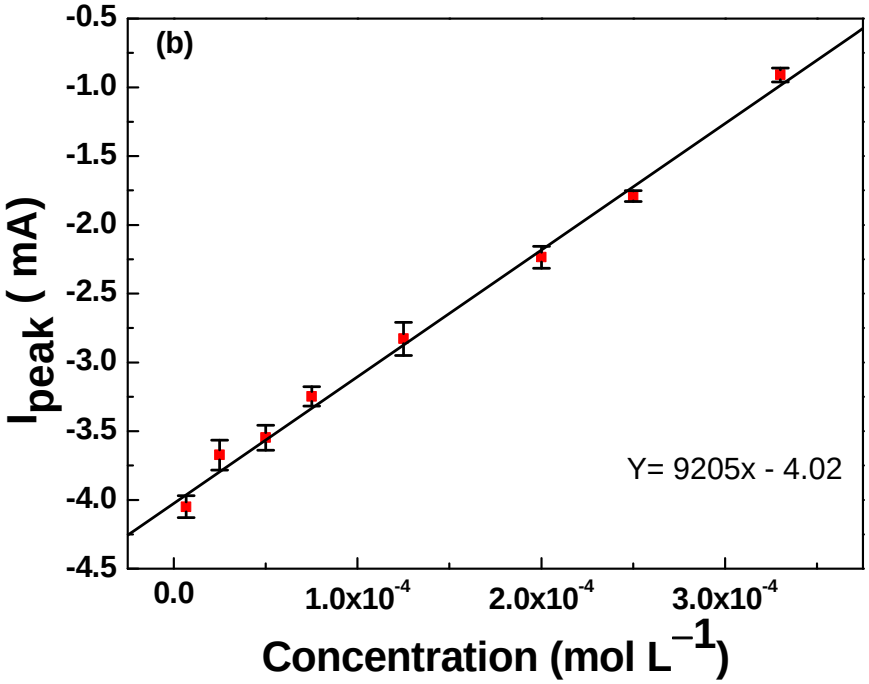

Figure 5. a) Linear sweep voltammetry curves registered for increasing concentrations of urea ranging from 6.66 x 10^{-6} to 3.33 x 10^{-4} mol L^{-1} in KCl 0.10 mol L^{-1}. (b) Linear relationship between the registered I_{peak} versus the concentration of urea showing excellent fitting for linear relationship. LSV curves of were registered on Ti/RuO_2-TiO_2-SnO_2 (50:40:10 atom. %) working electrode at υ = 50 mV s^{-1} scan rate after holding 1.2 V vs Ag/AgCl for 60 seconds as analytical preconditioning.

Table 4. Analytical features obtained for LSV urea determination.

Performance characteristics*	**Urea**
Linear range (mol L^{-1})	6.66×10^{-6} to 3.33×10^{-4}
Intercept	-4.02 ± 0.004
Sensitivity (mA mol L^{-1})	9205 ± 0.004
LOQ (mol L^{-1})	7.66×10^{-6}
LOD (mol L^{-1})	1.83×10^{-6}
R^2	0.997
Repeatability (RSD for n = 32)	5.10%
Reproducibility (RSD for n=7)	1.81%

*LOD: limit of detection; LOQ: limit of quantification; RSD: relative standard deviation.

If we compare these highly promising results (Table 4) with previous literature reports showed in Table 5, the proposed electrochemical quantification of urea by Ti/RuO_2-TiO_2-SnO_2 (50:40:10 atom. %) outperforms other electroanalytical approaches in terms of LOD, linearity, stability and reproducibility. The repeatability and reproducibility tests showed low standard deviations, which indicates a good agreement between the analyses performed these materials. Thus, the DSA produced in the present work demonstrates an excellent efficiency linking the qualities of being an easily produced electrode and the ability to detect and quantify urea in a simple and fast way.

Table 5. Comparison between performance characteristics of the proposed method and other studies described in the literature for urea determination.

Electrode	**Technique***	**Linear Range (mol L^{-1})**	**LOD (mol L^{-1})**	**Ref.**
AgNP-deposited commercial Au-Pd electrode	CV	1.66×10^{-4} to 1.67×10^{-3}	0.141	38
Au electrode deposited with Ni	CV	-	0.033	39
Glassy carbon modified with nickel sulfide/graphene oxide	DPV	9.99×10^{-3} to 0.049	3.80×10^{-3}	40
3D graphene/$NiCo_2O_4$	CA	0.049 to 0.249	2.66×10^{-3}	41
NiO/celulose/CNT	CA	9.99×10^{-3} to 1.40	3.78×10^{-3}	42
Ti/RuO_2-TiO_2-SnO_2	LSV	6.66×10^{-6} to 3.33×10^{-4}	1.83×10^{-6}	**This work**

*DPV: Differential pulse voltammetry; CA: chronoamperometry.

It was analyzed the presence of several metal ions that can interfere in the urea analysis [43,44]. The interferents were analyzed in the proportions of 1:1 (interferent: urea) and it showed a loss (-) and current gain (+) as a percentage. The results obtained are shown in Table 6.

Table 6. Effects of additions of some interferents on the LSV signals of 3.33 mol L^{-1} of urea in 0.1 mol L^{-1} KCl solution.

Interferents	Current signal variation (%) Interferent:Analyte ratio 1:1
Ni(II)	-8.2
Zn(II)	+9.7
S(II)	−13.2
Cd(II)	-20.0
Fe(III)	−20.4
Pb(II)	-22.4
Cu(II)	−25.0

Table 6 shows that nickel(II), zinc(II) ions did not significantly interfere with the analytical urea signal, considering the tolerable limit of ±10% for interference [45]. The results obtained from sulfur(II) and iron(II) ions showed decreased analytical signals in current. According to Wilson et al. 2019, this may be due to metallic species suffer oxidation in the presence of electrogenerated active chlorine in situ [46]. In addition, cadmium(II), lead(II), and copper(II) ions showed decreased analytical signals in current as similarly reported elsewhere [47-48]. This can be related to the lower generation of active chlorine species due to their ability to complex chloride. Note that any aspect of the system that conditions the electrogeneration of active chlorine species (our indirect measure) it can decrease the overall peak signal registered during the cathodic scan.

In order to discuss a real scenario, we conducted analyses with synthetic urine samples. After obtaining the analytical parameters of the sensor Ti/RuO_2-TiO_2-SnO_2 (50:40:10 atom. %), the method proposed was applied for the analysis in a complex sample of synthetic urine. The analyses of synthetic urine samples were prepared containing 2.77 x 10^{-4} mol L^{-1} of urea in 0.10 mol L^{-1} KCl. The final concentration of urea found using the DSA electrode following the indirect electroanalytical method was 3.31 x 10^{-4} mol L^{-1} with an error estimated at +16%, which is acceptable for an online measurement that provides a continuous evaluation of urine in real effluents. These results can be related to the presence of interferents in synthetic urine as discussed during the study of effect of coexisting species.

4. Conclusions

This proof of concept demonstrates that Ti/RuO_2-TiO_2-SnO_2 (50:40:10 atom. %) DSA electrodes can be used for indirect electrochemical quantification of urea. The preparation method of mixed metal oxide electrodes allowed to obtain a morphological composition of tetragonal RuO_2 and anatase TiO_2 with solid solution of ruthenium and tin atoms into the TiO_2 structure. The mud-cracked morphology of the electrode was characteristic of mixed metal oxides and in good agreement with other reports in the literature. The CV analyses allowed to infer that urea was oxidized by electrogenerated active chlorine species. The usage of electrogenerated active chlorine species was directly correlated the target analyte concentration. This indirect method was translated to a LSV measurement with a 60 s induction time for active chlorine electrogeneration prior electroanalytical sensing. The method developed presents an LOD = 1.83 x 10^{-6} mol L^{-1} for urea in solution. Therefore, it is demonstrated through this proof of concept that indirect electroanalytical quantification of urea can be conducted using DSA electrodes by exploiting their characteristic catalytic feature (*i.e.*, high activity for chlorine evolution). Thus, it is feasible to indirectly quantify simply and quickly the presence of urea by reducing electrogenerated chlorine without the need for large amounts of sample and reagents.

Supplementary Materials: None

Author Contributions: Conceptualization, V.M.L.; S.L.R.; and R.J; methodology, V.M.L.; S.L.R.; and L. C-S.; data curation, V.M.L; and L. C-S.; writing—original draft V.M,L.; writing—review and editing, R.J.; G-S.S; F.A.S; supervision, R.J. All authors read and approved the final manuscript.

Funding: This research was funded by Coordenação de Aperfeiçoamento de Pessoal de Nível Superior—Brasil (CAPES); Fundação de Amparo à Pesquisa e Inovação do Espírito Santo (FAPES); Conselho Nacional de Desenvolvimento Científico e Tecnológico (CNPq); Universidade Federal do Espírito Santo (UFES). A.S. Fajardo and S. Garcia-Segura acknowledge the support received from the European Union's Horizon 2020 research and innovation program under the Marie Sklodowska-Curie grant agreement No 843870. This work was partially funded by the National Science Foundation (NSF) through the Nanotechnology-Enabled Water Treatment Nanosystems Engineering Research Center under project EEC-1449500.

Institutional Review Board Statement: Not applicable.

Informed Consent Statement: Not applicable

Data Availability Statement: Data is contained within the article.

Conflicts of Interest: The authors declare no conflict of interest.

References

1. Erfkamp, J, M.; Guenther, G. Gerlach. Enzyme-functionalized piezoresistive hydrogel biosensors for the detection of urea. *Sensors* **2019**, 19, 2858. https://doi.org/10.3390/s19132858.
2. Li, L.; Long, Y.; Gao, J.-M.; Song, Yang, K.G. Label-free and pH-sensitive colorimetric materials for the sensing of urea. *Nanoscale* **2016**, 8, 4458–4462. 10.1039/C5NR07690K
3. Fiorillo, A.S.; Tiriolo, R.; Pullano, S.A. Absorption of urea into zeolite layer integrated with microelectronic circuits. *TNANO* **2015,** 14, 214–217. 10.1109/tnano.2014.2378892
4. Pundir, C.S.; Jakhar, S.; Narwal, V. Determination of urea with special emphasis on biosensors: A Review. Biosensors and Bioelectronics **2018**, 123, 36-50. https://doi.org/10.1016/j.bios.2018.09.067
5. Rahmanian, R.; Mozaffari, S.A.; & Abedi, M. Disposable urea biosensor based on nanoporous ZnO film fabricated from omissible polymeric substrate. *Mater. Sci. Eng.* C **2015**, 57, 387–396. https://doi.org/10.1016/j.msec.2015.08.004
6. Hilding-Ohlsson, A.; Fauerbach, J.A.; Sacco, N.J.; Bonetto, M.C.; Cortón, E. Voltamperometric discrimination of urea and melamine adulterated skimmed milk powder. *Sensors* **2012**, 12, 12220–12234. https://doi.org/10.3390/s120912220
7. Manjakkala, L.; Szwagierczakb, D.; Dahiya, R. Metal oxides based electrochemical pH sensors: Current progress and future perspectives. *Prog. Mater. Sci.* **2020**, 109, 100635. https://doi.org/10.1016/j.pmatsci.2019.100635.
8. Li, S.; Simonian, A.; Chin, B.A. Sensors for agriculture and the food industry. *Electrochem. Soc. Interface.* **2010**, 19, 41–46. https://doi.org/10.1149/2.F05104if.
9. Zhuiykov, S. Solid-state sensors monitoring parameters of water quality for the next generation of wireless sensor networks. *Sens Actuat B.* **2012**, 16, 1–20. https://doi.org/10.1016/j.snb.2011.10.078.
10. Grgur, B.N. Electrochemical oxidation of bromides on DSA/RuO_2 anode in the semi-Industrial batch reactor for on-Site water disinfection. *JES.* **2019**, 166 , E50–E61. https://doi.org/10.1149/2.1391902jes.
11. Wang, L.; Morison, K. Implementation of online security assessment. *IEEE.* **2006**, 4, 46-59. 10.1109/MPAE.2006.1687817.
12. Nakamura, K.C.; Guimarães, L.S.; Magdalena, A.G.; Angelo, A.C.D.; de Andrade, A.R; Garcia-Segura, S.; Pipi, A.R.F. Electrochemically-driven mineralization of Reactive Blue 4 cotton dye: On the role of in situ generated oxidants. *J. Electroanal. Chem.* **2019**, 840, 415–422. https://doi.org/10.1016/j.jelechem.2019.04.016.
13. Garcia-Segura, S.; Nienhauser, A.B.; Fajardo, A.S.; Bansal, R.; Coonrod, C.L.; Fortner, J.D.; Marcos-Hernández, M.; Rogers, T.; Villagran, D.; Wong, M.S.; Westerhoff, P. Disparities between experimental and environmental conditions: research steps toward making electrochemical water treatment a reality. *Curr. Opin. Electrochem.* **2020**, 22, 9–16. https://doi.org/10.1016/j.coelec.2020.03.001.
14. Trasatti, S. Electrocatalysis in the anodic evolution of oxygen and chlorine. *Electrochim. Acta.* **1984**, 29, 1503–1512. https://doi.org/10.1016/0013-4686(84)85004-5.

15. Trieua, V.; Schleya, B.; Natter, H.; Kintrup, J.; Bulan, A.; Hempelmanna, R. RuO_2-based anodes with tailored surface morphology for improved chlorine electro-activity. *Electrochim. Acta.* **2012**, 78, 188–194. https://doi.org/10.1016/j.electacta.2012.05.122.
16. Papulova, G.N.; Kvasnikov, M. Yu. Water-soluble urea-formaldehyde oligomers in paint for single-firing decoration of ceramic. *Glass and Ceram.* **2020**, 77, 3–4. https://doi.org/10.1007/s10717-020-00252-1.
17. Kapałka, A.; Katsaounis, A.; Michels, N-L.; Leonidova, A.; Souentie, S.; Comninellis, C.; Udert, K.M. Ammonia oxidation to nitrogen mediated by electrogenerated active chlorine on Ti/PtO_x-IrO_2. *Electrochem. Commun.* **2010**, 12, 1203-1205. https://doi.org/10.1016/j.elecom.2010.06.019.
18. Carneiro, J.F.; da Silva, J.R; Rocha, R.S.; Ribeiro, J.; Lanza, M.R.V. Morphological and electrochemical characterization of Ti/$M_xTi_ySn_zO_2$ (M = Ir or Ru) electrodes prepared by the polymeric precursor method. *Adv. Chem. Enginner. Sci.* **2016**, 06 , 364-378. 10.4236/aces.2016.64037.
19. Ribeiro, J.; Alves, P.D.P.; de Andrade, A.R. Effect of the preparation methodology on some physical and electrochemical properties of Ti/$Ir_xSn_{(1-x)}O_2$ materials. *J. Mater. Sci.* **2007**, 42, 9293–9299. https://doi.org/10.1007/s10853-007-1906-1.
20. Manjakkal, L.; Cvejin, K.; Kulawik, J.; Zaraska, K.; Szwagierczak, D.; Stojanovic, G. Sensing mechanism of RuO_2–SnO_2 thick film pH sensors studied by potentiometric method and electrochemical impedance spectroscopy. *J. Electroanal. Chem.* **2015**, 759, 82–90. https://doi.org/10.1016/j.jelechem.2015.10.036.
21. Shin, Y.-U.; Yoo, H.-Y.; Kim, S.; Chung, K.-M.; Park, Y.-G.; Hwang, K.-H.; Hong, S.W.; Park, H.; Cho, K.; Lee, J. Sequential combination of electro-fenton and electrochemical chlorination processes for the treatment of anaerobically-digested food wastewater. *Environ. Sci. Technol.* **2017**, 51, 10700–10710. 10.1021/acs.est.7b02018.
22. Neto, S.A.; de Andrade A.R. Electrooxidation of glyphosate herbicide at different DSA® compositions: pH, concentration and supporting electrolyte effect. *Electrochim. Acta.* **2009**, 54, 2039–2045. https://doi.org/10.1016/j.electacta.2008.07.019.
23. Lopez-Ojeda, G.C.; Gutierrez-lara, Ma. R.; Duran-Moreno, A. Efecto del pH sobre la oxidación electroquímica de fenol empleando un ánodo dimensionalmente estable de SnO_2-Sb_2O_5-RuO_2. *Rev. Mex. Ing. Quím.* **2015**, 14, 437-452.
24. Crittenden, J.C.; Trussell, R.R.; Hand, D.W.; Howe, K.J.; Tchobanoglous, G. Water Treatment Principles and Design, 3rd ed. Wiley.; New Jersey, 2012, pp. 532-542.
25. Garcia-Segura, S.; Mostafa, E.; Baltruschat, H. Electrogeneration of inorganic chloramines on boron-doped Diamond anodes during electrochemical oxidation of ammonium chloride, urea and synthetic urine matrix. *Water Res.* **2019**, 16, 0107-117. https://doi.org/10.1016/j.watres.2019.05.046.
26. Deroco, P.B.; Vicentini, F.C.; Oliveira, G.G.; Rocha-Filho, R.C.; Fatibello-Filho, O. Square-wave voltammetric determination of hydroxychloroquine in pharmaceutical and synthetic urine samples using a cathodically pretreated boron-doped diamond electrode. *J. Electroanal. Chem.* **2014**, 719, 19–23. http://dx.doi.org/10.1016/j.jelechem.2014.01.037
27. Laube, N.; Mohr, B.; Hesse. Laser-probe-based investigation of the evolution of particle size distributions of calcium oxalate particles formed in artificial urines. *A. J. Cryst. Growth* **2001**, 233, 367–374. https://doi.org/10.1016/S0022-0248(01)01547-0
28. Dbira, S.; Bensalah, N.; Cañizares, P.; Rodrigo, M.A.; Bedoui, A. The electrolytic treatment of synthetic urine using DSA electrodes. *J. Electroanal. Chem.* **2015**, 744, 62–68. http://dx.doi.org/10.1016/j.jelechem.2015.02.026
29. Cullity, B.D. Elements of x-Ray Diffraction, 3rd ed.; Addison-Wesley: San Francisco, CA, USA, 2001, pp. 99-106.
30. Comninellis, C.; Vercesi, G. P. Characterization of DSA| oxygen evolving electrodes: choice of a coating. J. Appl. *Electrochem.* **1991,** 21, 335-345. https://doi.org/10.1007/BF01020219.
31. Coteiro, R.D.; Teruel, F.S.; Ribeiro, J.; De Andrade, A. R. Effect of Solvent on the Preparation and Characterization of DSA®-Type Anodes Containing RuO_2-TiO_2-SnO_2. *J. Braz. Chem. Soc.* **2006**, 17, 771-779. https://doi.org/10.1590/S0103-50532006000400020.
32. Hutchings, R.; Müller, K.; Kötz, R.; Stucki, S. A Structural investigation of stabilized oxygen evolution catalysts. *J. Mater. Sci.* **1984**, 19, 3987– 3994. https://doi.org/10.1007/BF00980762.

33. Srinivasan, N.; Kiruthika, G.V.M. Conductivity studies on the substituted stannate pyrochlore system $Gd_2Sn_{2-xy}M_xA_yO_7$ (M= Ti and A = Ru; x = 0.5, 1.0 and 1.5; y = 0.2). *Solid State Sci.* **2019**, 96, 105957. https://doi.org/10.1016/j.solidstatesciences.2019.105957.
34. Kolesnikov, V.A.; Novikov, V.T.; Isaev, M.K.; Alekseeva, T.V.; Kolesnikov, A.V. Investigation of Electrodes with an Active Layer of a Mixture of the Oxides TiO_2, RuO_2, SnO_2. *Glass and Ceram.* **2018,** 75, 148–153. https://doi.org/10.1007/s10717-018-0045-2.
35. Ribeiro, J.; de Andrade, A.R. Characterization of RuO_2-Ta_2O_5 coated titanium electrode microstructure, morphology, and electrochemical investigation. *J. Electrochem. Soc.* **2004**, 151, 106-112. https://doi.org/10.1149/1.1787174.
36. Zeradjanin, A. R.; Schilling, T.; Seisel, S.; Bron, M.; Schuhmann, W. Visualization of chlorine evolution at dimensionally stable anodes by means of scanning electrochemical microscopy. *Analytical Chem.* 2011, 83, 7645–7650. https://doi.org/10.1021/ac200677g.
37. Bulska, E. Metrology in Chemistry, 1rd ed.; Springer: Cham, Switzerland, 2018, pp. 109-110.
38. Liu, J.; Moakhar, R.S.; Perumal, A.S.; Roman, H.N.; Mahshid, S.; Hogiu, S.W. An AgNP-deposited commercial electrochemistry test strip as a platform for urea detection. *Nature.* **2020**, 10, 9527. https://doi.org/10.1038/s41598-020-66422-x
39. Irzalinda, A.D.; Gunlazuardil, J.; Wibowo, R. Development of a non-enzymatic urea sensor based on a Ni/Au electrode. *J. Phys. Conf. Ser.* **2020**, 1442 012054. https://doi.org/10.1088/1742-6596/1442/1/012054.
40. Naik, T.S.S.K.; Saravanan, S.; Saravana, K.N.S.; Pratiush, U.; Ramamurthy, P.C. A non-enzymatic urea sensor based on the nickel sulfide/graphene oxide modified glassy carbon electrode. *Mater. Chem. Phys.* **2020**, 245 , 122798. https://doi.org/10.1016/j.matchemphys.2020.122798.
41. Nguyen, N.S.; Das, G.; Yoon, H.H. Nickel/cobalt oxide-decorated 3D graphene nanocomposite electrode for enhanced electrochemical detection of urea. *Biosens. Bioelectron.* **2016**, 77, 372–377. https://doi.org/10.1016/j.bios.2015.09.046.
42. Nguyen, N. S.; Yoon, H. H. Nickel oxide-deposited cellulose/CNT composite electrode for non-enzymatic urea detection. *Sensor Actuat. B-Chem.* **2016**, 236, 302-310. https://doi.org/10.1016/j.snb.2016.05.165.
43. Gimeno-García, E.; Andreu, V.; Boluda, R. Heavy metals incidence in the application of inorganic fertilizers and pesticides to rice farming soils. *Environmental Pollution* **1996**, 92, 19–25. https://doi.org/10.1016/0269-7491(95)00090-9.
44. Yaseen, D.A.; Scholz, M. Textile dye wastewater characteristics and constituents of synthetic effluents: a critical review. *IJEST* **2018**, 16, 1193–1226. https://doi.org/10.1007/s13762-018-2130-z.
45. Squissato, A.L.; Richter, E.M.; Munoz, R.A.A. Voltammetric determination of copper and tert-butylhydroquinone in biodiesel: A rapid quality control protocol. *Talanta* **2019**, 201, 433-440. https://doi.org/10.1016/j.talanta.2019.04.030.
46. Wilson, R.E.; Stoianov, I.; O'Hare, D. Continuous Chlorine Detection in Drinking Water and a Review of New Detection Methods. *Johnson Matthey Technol. Rev.*, **2019**, 63, 103–118. https://doi.org/10.1595/205651318X15367593796080.
47. Syshchyk, O.; Skryshevsky, V.A.; Soldatkin, O.O.; Soldatkin, A.P. Enzyme biosensor systems based on porous silicon photoluminescence for detection of glucose, urea and heavy metals. *Biosens. Bioelectron.* **2015**, 66, 89–94. https://doi.org/10.1016/j.bios.2014.10.075.
48. Lee, H-S.; Kim, C-K.. Determination of heavy metal ions using conductometric biosensor based on sol-gel immobilized urease. *Bull Korean Chem Soc*. 23, 1169–1172. https://doi.org/10.5012/BKCS.2002.23.8.1169.